HHS Public Access

Author manuscript

Mod Pathol. Author manuscript; available in PMC 2019 April 05.

Published in final edited form as:

Mod Pathol. 2019 March ; 32(3): 396–404. doi:10.1038/s41379-018-0148-x.

Identification of a Subset of Microsatellite-Stable Endometrial Carcinoma with High PD-L1 and CD8+ Lymphocytes

Suzanne Crumley, MD[1], **Katherine Kurnit, MD**[2], **Courtney Hudgens, BS**[1,4], **Bryan Fellman**[3], **Michael T. Tetzlaff, MD, PhD**[1,4], and **Russell Broaddus, MD, PhD**[1]

[1]Department of Pathology, The University of Texas M.D. Anderson Cancer Center, Houston, Texas, USA

[2]Department of Gynecologic Oncology and Reproductive Medicine, The University of Texas M.D. Anderson Cancer Center, Houston, Texas, USA,

[3]Department of Biostatistics, The University of Texas M.D. Anderson Cancer Center, Houston, Texas, USA

[4]Department of Translational and Molecular Pathology, The University of Texas M.D. Anderson Cancer Center, Houston, Texas, USA

Abstract

Immune checkpoint blockade has emerged as an effective therapeutic strategy for patients with advanced cancer. Identification of biomarkers associated with treatment efficacy will help to select patients more likely to respond to this approach. High levels of microsatellite instability, tumor expression of PD-L1, high tumor mutation burden, and increased tumor infiltrating lymphocytes have all been associated with response to checkpoint inhibitor blockade. The purpose of this study was to determine if a subset of microsatellite stable endometrioid endometrial carcinomas have higher immune cell infiltrates and/or expression of PD-L1. PD-L1 expression and characterization of immune cell infiltrates were analyzed in 132 microsatellite stable, FIGO grade 2 endometrioid carcinomas. PD-L1 was positive in 48% (63/132) of the tumors. Tumor cell expression of PD-L1 was significantly associated with lymphatic/vascular invasion and deep myometrial invasion. PD-L1 expression was especially prominent at the invasive front and in foci of tumor-associated squamous metaplasia. Twenty-one cases (16% of the total) with more diffuse and/or especially strong PD-L1 expression were identified. This PD-L1 high subset was associated with significantly higher numbers of tumor-associated CD3+ and CD8+ lymphocytes. Only one tumor in the PD-L1 high subset harbored a *POLE* mutation. PTEN immunohistochemical loss, a common event in endometrioid-type endometrial carcinoma and associated with local immune suppression in melanoma, was not associated with PD-L1 expression or lymphocyte/macrophage infiltration of the tumor. These results suggest that a subset of microsatellite-stable endometrial

Corresponding author: Russell Broaddus, MD, PhD, Department of Pathology, Unit 85,1515 Holcombe Blvd, Houston, TX, 77030, USA. rbroaddus@mdanderson.org.

Disclosures: none

This original research was presented in part at the United States and Canadian Academy of Pathology Annual Meeting, March 4–10, 2017, San Antonio, TX.

cancers has higher expression of PD-L1 and increased tumor-associated CD3+ and CD8+ lymphocytes, characteristics more commonly associated with endometrial cancers with high levels of microsatellite instability. These results suggest that screening strategies to select only microsatellite instability-high advanced endometrial cancers for checkpoint inhibitor therapy might exclude patients who could potentially benefit from this therapeutic approach.

Keywords

endometrial cancer; PD-L1; PTEN; microsatellite stable

Introduction

Endometrial cancer can be classified into four molecular clusters, including the ultramutated (characterized by mutation in the gene polymerase epsilon, *POLE*), hypermutated (characterized by high levels of microsatellite instability), copy number low (characterized by absence of *POLE* and *TP53* mutations and absence of microsatellite instability-high), and copy number high (characterized by presence of *TP53* gene mutations) clusters (1). Two of these groups (*POLE* and microsatellite instability-high) are associated with a high predicted mutational load. The neoantigens generated by the high mutational load in these tumors have been shown to elicit a more robust host immune response (2, 3). Both of these groups are associated with higher tumor-associated immune cells than the tumors in the microsatellite-stable group (2–5). Similarly, PD-L1 expression has been demonstrated to be higher in mismatch repair-deficient endometrial carcinomas compared to mismatch repair intact tumors (4–6). Therefore, much of the attention of immunotherapy research and clinical trials has focused on the microsatellite instability-high and *POLE*-mutated tumors (4–7).

While microsatellite instability is routinely measured in many clinical pathology laboratories, *POLE* is not commonly interrogated by most clinically available next-generation sequencing hotspot panels. Quantifying tumor mutation burden typically requires whole exome sequencing or, at the very least, a sequencing panel of several hundred genes. Thus, most clinical labs lack effective means to assess tumor mutation burden. A complicating issue is that not all tumors with high mutation burdens have *POLE* mutation or high levels of microsatellite instability (8). For endometrial cancer, it was recently shown that elevated predicted neoantigen load was associated with better prognosis in the TCGA copy number low endometrioid group and in the copy number high serous-like group; neither of these groups is associated with *POLE* mutation or microsatellite instability-high (9). These results suggest that in addition to the *POLE* mutated and microsatellite instability-high endometrial cancers, there are specific subsets of hypomutated endometrial cancer that may be more immunogenic and have improved outcomes and potentially better response to immunotherapy. Therefore, the purpose of the current study was to determine if a subset of microsatellite-stable/mismatch repair intact endometrial cancers exhibit increased tumor cell expression of PD-L1 expression and an immune microenvironment with increased numbers of tumor associated immune cells.

Materials and Methods

Patient Selection

The study was approved by the University of Texas MD Anderson Cancer Center's institutional review board (Protocol LAB01–718). Retrospective review from January 1, 2013 – May 5th, 2016 revealed 382 consecutive cases of endometrial carcinoma with available tissue that had previously been tested for DNA mismatch repair protein immunohistochemistry and/or microsatellite instability. It has been shown that endometrial tumor histology can influence PD-L1 expression, with higher expression observed in grade 3 endometrioid and non-endometrioid histologies (10). To minimize any possible variation in immune cell infiltrate that could be attributed to the histotype or grade of tumor, we selected for further examination FIGO grade 2 endometrioid carcinomas, as this was the most common histotype. A total of 132 microsatellite-stable, FIGO grade 2 endometrial endometrioid cancers with intact immunohistochemical expression of MLH1, MSH2, MSH6, and PMS2 were identified for further study (Figure 1). Tumor histotype was verified by light microscopic examination of H&E stained slides. Clinical and pathological variables, including, patient age, tumor size, myometrial invasion (less than or greater than 50%), lymphovascular space invasion, and tumor stage, were derived from the electronic medical record and pathology reports.

Assessment of DNA mismatch repair

Mismatch repair protein and microsatellite instability testing were performed according to methodology previously described (11). Immunohistochemistry of mismatch repair proteins was performed using standard techniques for MLH1 (G168–15 1:25; BD Biosciences Pharmingen), MSH2 (FE11, 1:100; Calbiochem), MSH6 (44, 1:300; BD Biosciences Pharmingen), and PMS2 (Alb-4, 1:125; BD Biosciences Pharmingen). Immunohistochemistry was scored as mismatch repair protein intact or deficient using light microscopic examination. Complete absence of mismatch repair protein expression was required in order for a case to be designated as mismatch repair deficient. Stromal cells served as an internal positive control. PCR-based microsatellite instability analysis was performed using 7 microsatellites (TGFBR2 and the 6 National Cancer Institute recommended microsatellites, BAT25, BAT26, BAT40, D2S123, D5S346, and D17S250). A tumor was considered microsatellite instability-high if three or more of the seven markers demonstrated allelic shift. Tumors without allelic shift were designated as microsatellite stable.

Immunohistochemistry

Immunohistochemistry was performed on a Leica Bond autostainer with the following antibodies and 3,3'-diaminobenzidine chromogen: CD3 (Dako AO452, 1:100), CD8 (Life Sciences Technology MS457s, 1:25), CD68 (Dako PG-M1, 1:450), programmed death ligand-1 (PD-L1; Cell Signaling Technology 13684S, clone E13N, 1:100), PTEN (Dako, clone 6H2.1, 1:100), p53 (Dako, clone D0–7, 1:100), and β-catenin (BD Biosciences, clone 14, 1:1500). Immunohistochemistry for PTEN, PD-L1, p53, and β-catenin was assessed by light microscopic examination. PTEN staining was classified as positive, negative, or heterogeneous, with adjacent stromal cells serving as an internal positive control (12; Figure

1). PD-L1 expression was characterized in tumor cells and classified as 1+ (faint), 2+ (moderate), and 3+ (strong) as well as the percentage of positive staining present. A subgroup of cases with either 2% or greater percentage of staining in the tumor and/or 3+ tumor positivity was considered as the “tumor PD-L1 high positive” subgroup. We focused primarily on PD-L1 expression in tumor cells, rather than expression in stroma or tumor-associated inflammatory cells, as tumor cell PD-L1 expression is associated with response to anti-PD-1 therapy (13), and there is poor inter-observer agreement for interpretation of PD-L1 in tumor-associated immune cells (14). This PD-L1 antibody clone (E13N) has been recently shown to have comparable performance characteristics as the FDA-approved companion diagnostic assays employing clones 22c3 and 28–8 (14). Any nuclear expression of β-catenin by light microscopy is highly associated with the presence of an exon 3 *CTNNB1* gene mutation (15). For p53 immunohistochemistry, scattered nuclear staining in the tumor is correlated to *TP53* gene wildtype, while strong, diffuse nuclear expression or complete lack of nuclear staining is associated with *TP53* gene mutation (summarized for endometrial cancer in 16).

Tumor-associated immune cell infiltrate analysis

Immunohistochemistry with antibodies for CD3 (lymphocytes), CD8 (lymphocytes), and CD68 (macrophages) was used to determine the composition, density, and distribution of the tumor-associated immune cell infiltrates. Immunohistochemical stained slides were analyzed using image analysis software (Aperio ImageScope) in order to quantify the number of positive cells within designated areas. Slides were scanned at 20X (Aperio Scanscope AT Turbo; Leica Biosystems) utilizing methods previously described (17). The areas of highest positive cell density for each immune cell marker were identified by placement of five 1 mm^2 boxes in the center of the tumor and along the periphery/leading edge of the tumor (Figure 2). The periphery/leading edge of the tumor was defined as +/− 1 mm from the invasive tumor front (if present) or +/− 1 mm from the endometrial-myometrial interface. The center of the tumor was defined as the area greater than 1 mm towards the luminal aspect from the endometrial-myometrial interface or invasive tumor front (Figure 2). Therefore, for both the tumor periphery and center, a total of 5 mm^2 areas containing the highest density of CD3-, CD8-, or CD68- positive cells were identified. The single highest density box among these was designated as the hotspot for each immune cell marker. “Overall” was defined as the combined sum of the positive cells tabulated along the tumor periphery and within the tumor center. For each region (periphery, center, hotspot, and overall), the number of total positive cells was added and divided by the total area (mm^2) in which the cells were counted. The results for CD3, CD8, and CD68 were reported as number of positive cells/mm^2.

POLE Mutational Analysis

The cases designated as tumor PD-L1 high (n=21) were tested by Sanger sequencing for mutation in the exonuclease domain of DNA polymerase ε (*POLE*; exons 9–14) (18). Microdissected sections from formalin-fixed, paraffin-embedded tumor were used for sequencing. DNA was extracted using the Pico Pure DNA extraction kit (Applied Biosystems).

Statistical Analysis

Demographic and clinical characteristics for all patients were summarized with descriptive statistics. Characteristics were compared by tumor PD-L1 status (negative vs. positive; negative vs high positive). Wilcoxon rank-sum test was used to compare continuous variables, and chi –squared or Fisher's exact test was used to compare categorical variables. A Bonferroni correction was used to control the false discovery rate within each of the main comparisons. Statistical significance threshold was defined at 0.0025 (0.05/20). All statistical analyses were conducted using Stata v14.1 (College Station, TX).

Results

The clinical and pathological characteristics for the 132 cases of mismatch repair intact endometrial endometrioid adenocarcinoma, FIGO Grade 2, are summarized in Table 1. The median patient age was 60 years. The majority of patients presented with early stage disease (stage I or II, 89% of patients).

PD-L1 was positive in 48% (63/132) of the tumors. The majority of cases had weaker 1–2+ PD-L1 staining (55/63, 87%) and/or PD-L1 staining was very focal, staining 1% of the tumor (43/63, 68%). Tumor cell expression of PD-L1 was associated with deeper myometrial invasion and the presence of lymphatic/vascular space invasion in the hysterectomy (Table 2). Both advanced tumor stage (p=0.012) and PTEN loss (p=0.012) showed trends towards being associated with PD-L1 expression, but these differences were not statistically significant given the threshold of 0.0025 to control for false discovery with multiple comparisons (Table 2).

Despite controlling for endometrial cancer histotype (endometrioid), grade (FIGO 2), and having comparable mean patient ages for PD-L1 negative and PD-L1 positive groups, a broad spectrum of CD3+, CD8+, and CD68+ expression within the tumor was encountered. In general, CD3+ or CD8+ lymphocytes comprised most of the tumor-associated immune cell infiltrate, with smaller numbers of CD68+ macrophages (Table 2). The numbers of lymphocytes and macrophages did not differ significantly when comparing tumor center to tumor periphery (Table 2). Tumor cell expression of PD-L1 was not associated with significant differences in CD3+ or CD8+ tumor-associated lymphocytes, although the PD-L1 positive group showed trends towards higher numbers of these lymphocytes (Table 2). The number of CD68+ tumor-associated macrophages did not differ significantly according to PD-L1 expression (Table 2). Independent of PD-L1 expression, the presence of myometrial invasion, myometrial invasion ≥50% myometrial thickness, and lymphatic/vascular space invasion were not associated with significant changes in CD3+, CD8+, or CD68+ immune cell composition (data not shown).

Tumor cell expression of PD-L1 was especially prominent in foci of tumor squamous metaplasia, foci of myometrial invasion, and foci of lymphatic/vascular space invasion (Figure 2 C, D). When present, squamous differentiation appeared to be more strongly associated with PD-L1 expression. Absence of squamous differentiation was noted in 74% of the PD-L1 negative cases, but only in 29% of the PD-L1 positive cases. A subset of tumors (21/63 PD-L1 positive cases, 33%; 21/132 total cases, 16%) had higher PD-L1

expression, characterized as either increased percentage of tumor cells positively staining or the presence of 3+ staining intensity. Sixteen of 63 cases (25%) had 2–5% of tumor staining, 3 cases (5%) had 6–20% of tumor staining, and 1 case (2%) had 75% of tumor staining. One case with 1% of tumor staining positive for PD-L1 was included in the PD-L1 high subset because it had stronger intensity of staining (3+) in tumor cells. Only 10% of the tumors in the PD-L1 high subset lacked squamous differentiation, and in 86% of the PD-L1 high tumors the squamous portion was positive for PD-L1. Presence of PD-L1 high was associated with significantly increased CD3+ and CD8+ lymphocytes in the tumor hotspot and significantly increased CD3+ lymphocytes in the tumor periphery compared to PD-L1 negative cases (Table 3). The number of CD68+ macrophages was not significantly different between PD-L1 high and PD-L1 negative cases (Table 3). Higher levels of PD-L1 were not significantly associated with any of the other clinical or pathological variables studied (Table 3).

POLE mutation has been previously associated with increased tumor infiltrating lymphocytes (4). We hypothesized that because of its association with higher CD3+ and CD8+ lymphocytes, the PD-L1 high subset would be enriched with tumors with *POLE* mutation. However, only 1 mutation, a *POLE* exon 9 mutation, was identified in the PD-L1 high subset. This case was from a 60 year-old patient with a stage I, grade 2 endometrioid carcinoma with less than 50% myometrial invasion. Microscopically, this tumor did not have distinct features. Lymphatic/vascular space invasion was absent, and there was no metastasis in 12 surgically resected lymph nodes or the omentum. The tumor had 3+ strength of tumor staining for PD-L1 in approximately 3% of the tumor cells. The number of CD3+, CD8+, and CD68+ cells were not significantly higher in the one *POLE* mutant tumor compared to the *POLE* wildtype tumors (data not shown).

Higher expression of PD-L1 has been observed in grade 3 endometrioid and non-endometrioid carcinomas (10). As these histotypes are associated with *TP53* gene mutation and/or immunohistochemistry patterns suggestive of *TP53* gene mutation, we speculated that the PD-L1 high subset was enriched with tumors with *TP53* gene mutation. However, all of the 21 tumors in this subset had scattered, weak nuclear expression of p53, associated with *TP53* gene wildtype (data not shown). Seven of the 21 tumors in the PD-L1 high subset had nuclear localization of β-catenin, associated with *CTNNB1* gene mutation. The CD3+, CD8+, and CD68+ immune cell infiltrates in these 7 tumors were not significantly different compared to the 14 PD-L1 high cases without nuclear β-catenin (data not shown).

PTEN loss is one of the most common molecular events in endometrioid-type endometrial carcinoma (12). In the 132 carcinomas examined in this study, 45% had PTEN protein loss by immunohistochemistry (Table 1). In melanoma, PTEN loss is associated with fewer CD8+ lymphocytes at the tumor site, decreased T-lymphocyte-mediated cell death, and decreased response to PD-1 blockade (19). In the current study, PTEN loss was not significantly associated with expression of PD-L1 or PD-L1 high (Tables 2 and 3). Independent of tumor PD-L1 status, there were no significant differences in numbers of CD3+ lymphocytes, CD8+ lymphocytes, or CD68+ macrophages in PTEN positive vs. PTEN negative tumors (Table 4).

Discussion

Efforts to identify biomarkers associated with endometrial cancer patients most likely to respond to immune based therapeutic approaches are important. Endometrial cancer is the most common gynecologic malignancy, with an estimated 63,230 new diagnoses in 2018 (20). In contrast to many other common cancer types, incidence and annual deaths from endometrial cancer are increasing (20,21). There are few therapeutic options for women with advanced or recurrent endometrial cancer, and no new agents have been approved in the past few decades (22,23). Therefore, immune-based approaches, in carefully chosen patients, have the potential to make a real impact in this disease.

In this study, we identified a subset (16%) of microsatellite-stable, mismatch repair intact endometrioid type endometrial carcinomas with increased tumor PD-L1 immunohistochemical staining (PD-L1 high positive subgroup). The tumors with increased tumor PD-L1 expression also showed increased numbers of CD3+ and CD8+ lymphocytes. This PD-L1 high group was not enriched with *POLE* mutations. These findings support the idea proposed by Shukla et al. (9) that there is a subset of *POLE* wildtype, mismatch repair intact endometrial cancers with increased tumor-associated lymphocytes. As yet unknown molecular mechanisms may underlie the recruitment of immune cells to these particular endometrioid carcinomas. Data from immunotherapy clinical trials will be necessary to determine if this subset is also more responsive to this therapeutic approach.

Although PD-L1 expression has been shown to be more frequent in microsatellite instability-high/*POLE*-mutated endometrial cancer (4–6, 10), PD-L1 staining has also been reported in microsatellite-stable endometrial carcinoma. In recent studies, the reported percentage of mismatch repair intact endometrial carcinomas with tumor cell expression of PD-L1 ranged from 4–20% (4, 5, 10); this range is comparable to the percentage of PD-L1 high (16%) in the current study. The variable percentage of cases positive for PD-L1 may be due to varying methodologies, including different PD-L1 antibodies, inclusion of endometrioid versus non-endometrioid histologies, stochastic geographic differences in PD-L1 expression, as well as tissue sampling by microarray versus full tissue sections. To keep tumor histology constant, the current study only included patients with FIGO grade 2 endometrioid endometrial carcinomas. It has been previously shown that lower grade endometrioid tumors have lower PD-L1 expression compared to grade 3 endometrioid carcinomas and non-endometrioid carcinomas (10). The detection of any tumoral staining was higher in the current study (48%) as compared to these previous studies. This may be due, in part, to the fact that full tissue sections of tumor were used in the current study, as the staining by PD-L1 can be very focal (1% tumor cells positive in the majority of cases in this study). Given that we frequently observed positive PD-L1 tumor staining in the invasive front, inclusion of the periphery/invasive front should be considered if tissue microarray analyses are performed. Overall, the focal and weak PD-L1 staining in the majority of cases of mismatch repair intact endometrial cancers in our study is consistent with the results of previous published work.

The immunohistochemical expression characteristics of PD-L1 identified in this study provide useful insight into the staining pattern in endometrial cancer. Cancers with

metaplastic changes, such as squamous metaplasia, were noted to have increased PD-L1 staining (Figure 2). Tumor PD-L1 positivity was frequently noted in the invasive front in the tumor PD-L1 high subgroup. In addition, staining was noted more frequently in cases with lymphatic/vascular space invasion, which was also previously reported (10). This raises the possibility that the microcystic elongated fragmented pattern of endometrial cancer invasion (24) could be associated with PD-L1 expression, due to its morphologic associations with metaplastic changes and lymphatic/vascular space invasion. The current study was not optimally designed to examine any possible association between PD-L1 and this distinctive invasive pattern, as only 5% of the 132 endometrial cancers examined showed this invasion pattern. This relatively low percentage is likely due to the fact that 99/132 (75%) of the cases included in this study had no myometrial invasion or less than 50% myometrial thickness invasion (stage IA). The PD-L1 high subset was not associated with aberrant p53 tumor expression. Nuclear translocation of β-catenin did not preferentially occur in the PD-L1 high subset. Thus, other than the presence of squamous metaplasia, which is very common in endoometrioid carcinomas, and increased numbers of CD3 positive and CD8 positive lymphocytes, this PD-L1 high subset does not have distinctive clinical or pathological features. Based on these results, this subset would reside in the copy number-low TCGA group of endometrial cancers, which is the largest group (1).

Tumors with *POLE* mutation, high levels of microsatellite instability, or high tumor mutation burden all seem to have in common a higher tumor associated immune cell infiltrate. This is important, as evidence suggests that increased tumor associated immune cells is associated with better survival and improved responses to checkpoint inhibitor therapy. In a mouse model of melanoma, pre-treatment with a PI3Kβ inhibitor resulted in increased tumor T lymphocytes and improved responses to anti-CTLA-4 and anti-PD-1 therapy (19). Responders to PD-1 blockade have significantly increased density in CD3+, CD8+, and CD45RO+ T lymphocytes in melanoma (25). In colorectal adenocarcinoma, higher intra-tumoral CD8+ T cells are associated with objective response to pembrolizumab (7). Higher expression in the tumor of *CD8* mRNA is associated with higher *PD-L1* mRNA expression and significantly increased survival in endometrioid-type endometrial carcinoma (26). It has been argued that both increased tumor associated lymphocytes and increased PD-L1 expression on tumor cells are necessary for optimal response to checkpoint inhibitor blockade (13).

An emerging area of study is the concept that tumor associated mutations may act as molecular modifiers of immune cell function. PTEN loss has been shown to be associated with decreased CD8+ immune cells and resistance to anti-PD-1 therapy in melanoma (19). PTEN loss does not seem to be associated with increased PD-L1 expression in melanoma (19). It was proposed that PTEN loss and PD-L1 expression were occurring due to two separate mechanisms that evolved independently to influence the immune microenvironment. An association with PTEN loss and PD-L1 expression has been reported in other tumor types such as glioblastoma multiforme and colorectal cancer (27). In the current study, PTEN loss had no statistically significant impact on PD-L1 expression or the density of CD3, CD8, and CD68 tumor associated immune cells. This suggests that molecular modifiers of the local tumor immune response may be tumor type-specific. Using a pan-cancer analytic approach, tumor driver mutations in *CTNNB1*, *NRAS*, and *IDH1* have

been associated with lower levels of immune cells in tumors (28). *NRAS* and *IDH1* mutations are uncommon in endometrial cancer, but *CTNNB1* mutation occurs in approximately 20% of endometrioid endometrial carcinomas and has been associated with decreased recurrence-free survival (29,30). Activation of the Wnt/β-catenin pathway in melanoma is associated with local immune suppression (31). Such a mechanism of local immune suppression by *CTNNB1* mutation or activation of the Wnt/β-catenin pathway has not yet been described for endometrial cancer, but it could explain, at least in part, the worse survival in this group of patients.

Acknowledgments

Financial Support: NIH Research Training Grant (KCK) T32 CA101642; NIH SPORE in Uterine Cancer (RRB) NIH P50 CA09825; Cancer Center Support Grant (BF) NIH CA016672

References

1. Kandoth C, Schultz N, Cherniack AD, et al. Integrated genomic characterization of endometrial carcinoma. Nature 2013; 497: 67–73. [PubMed: 23636398]
2. Suemori T, Susumu N, Iwata T, et al. Intratumoral CD8+ lymphocyte infiltration as a prognostic factor and its relationship with cyclooxygenase 2 expression and microsatellite instability in endometrial cancer. Int J Gynecol Cancer 2015; 25: 1165–1172. [PubMed: 26111272]
3. van Gool IC, Eggink FA, Freeman-Mills L, et al. POLE proofreading mutations elicit an antitumor immune response in endometrial cancer. Clin Cancer Res 2015; 21: 3347–3355. [PubMed: 25878334]
4. Howitt BE, Shukla SA, Sholl LM, et al. Association of polymerase ε-mutated and microsatellite-instable endometrial cancers with neoantigen load, number of tumor-infiltrating lymphocytes, and expression of PD-1 and PD-L1. JAMA Oncol 2015; 1: 1319–1323. [PubMed: 26181000]
5. Pakish JB, Zhang Q, Chen Z, et al. Immune microenvironment in microsatellite instable endometrial cancers: hereditary or sporadic origin matters. Clin Cancer Res 2017; 23: 4473–4481. [PubMed: 28264871]
6. Sloan EA, Ring KL, Willis BC et al. PD-L1 expression in mismatch repair-deficient endometrial carcinomas, including Lynch syndrome-associated and MLH1 promoter hypermethylated tumors. Am J Surg Pathol 2017; 41: 326–333. [PubMed: 27984238]
7. Le DT, Uram JN, Wang H, et al. PD-1 blockade in tumors with mismatch-repair deficiency. N Engl J Med 2015; 372: 2509–2520. [PubMed: 26028255]
8. Chalmers ZR, Connelly CF, Fabrizio D, et al. Analysis of 100,000 human cancer genomes reveals the landscape of tumor mutational burden. Genome Med 2017; 9: 34. [PubMed: 28420421]
9. Shukla SA, Howitt BE, Wu CJ, Konstantinopoulos PA. Predicted neoantigen load in non-hypermutated endometrial cancers: correlation with outcome and tumor-specific genomic alterations. Gynecol Oncol Rep 2017; 19: 42–45. [PubMed: 28070553]
10. Li Z, Joehlin-Price AS, Rhoades J, et al. Programmed death ligand 1 expression among 700 consecutive endometrial cancers: strong association with mismatch repair protein deficiency. Int J Gynecol Cancer 2018; 28: 59–68. [PubMed: 29053481]
11. Bartley AN, Luthra R, Saraiya D, et al. Identification of cancer patients with Lynch Syndrome: clinically significant discordances and problems in tissue-based mismatch repair testing. Cancer Prev Res 2012; 5: 320–327.
12. Djordjevic B, Hennessy BT, Li J, et al. Clinical assessment of PTEN loss in endometrial carcinoma: immunohistochemistry outperforms gene sequencing. Mod Pathol 2012; 25: 699–708. [PubMed: 22301702]
13. Taube JM, Klein A, Brahmer JR, et al. Association of PD-1, PD-1 ligands, and other features of the tumor immune microenvironment with response to anti-PD-1 therapy. Clin Cancer Res 2014; 20: 5064–5074. [PubMed: 24714771]

14. Rimm DL, Han G, Taube JM, et al. A prospective, multi-institutional, pathologist-based assessment of 4 Immunohistochemistry assays for PD-L1 expression in non-small cell lung cancer. JAMA Oncol 2017; 3: 1051–1058. [PubMed: 28278348]
15. Kim G, Kurnit KC, Djordjevic B, et al. Nuclear β-catenin localization and mutation of the CTNNB1 gene: a context-dependent association. Mod Pathol 2018; i*n press*. doi 10.1038/s41379-018-0080-0
16. Malpica A How to approach the many faces of endometrioid carcinoma. Mod Pathol 2016; 29 suppl 1: S29–44. [PubMed: 26715172]
17. Feldmeyer L, Hudgens CW, Ray-Lyons G, et al. Density, distribution, and composition of immune infiltrates correlate with survival in Merkel cell carcinoma. Clin Cancer Res 2016; 22: 5553–5563. [PubMed: 27166398]
18. Billingsley CC, Cohn DE, Mutch DG, et al. Polymerase ε (*POLE*) mutations in endometrial cancer: clinical outcomes and implications for Lynch Syndrome testing. Cancer 2015; 121: 386–394. [PubMed: 25224212]
19. Peng W, Chen JQ, Liu C, et al. Loss of PTEN promotes resistance to T cell-mediated immunotherapy. Cancer Discov 2016; 6: 202–216. [PubMed: 26645196]
20. Siegel RL, Miller KD, Jemal A. Cancer Statistics, 2018. CA Cancer J Clin 2018; 68: 7–30. [PubMed: 29313949]
21. Jemal A, Ward EM, Johnson CJ, et al. Annual report to the nation on the status of cancer, 1975–2014, featuring survival. J Natl Cancer Inst 2017; 109: djx030.
22. MacKay HJ, Levine DA, Bae-Jump VL, et al. Moving forward with actionable therapeutic targets and opportunities in endometrial cancer: NCI clinical trials planning meeting report on identifying key genes and molecular pathways for targeted endometrial cancer trials. Oncotarget 2017; 8: 84579–84594. [PubMed: 29137450]
23. Lheureux S, Wilson M, MacKay HJ. Recent and current phase II clinical trials in endometrial cancer: review of the state of the art. Expert Opin Investig Drugs 2014; 23: 773–792.
24. Hertel JD, Huettner PC, Pfeifer JD. Lymphovascular space invasion in microcystic elongated and fragmented (MELF)-pattern well-differentiated endometrioid adenocarcinoma is associated with a higher rate of lymph node metastasis. Int J Gynecol Pathol 2014; 33: 127–134. [PubMed: 24487466]
25. Chen P-L, Roh W, Reuben A, et al. Analysis of immune signatures in longitudinal tumor samples yields insight into biomarkers of response and mechanisms of resistance to immune checkpoint blockade. Cancer Disc 2016; 6: 827–837.
26. Ikeda Y, Kiyotani K, Yew PY, et al. Clinical significance of T cell clonality and expression levels of immune-related genes in endometrial cancer. Oncol Rep 2017; 37: 2603–2610. [PubMed: 28358435]
27. Patel SP, Kurzrock R. PD-L1 expression as a predictive biomarker in cancer immunotherapy. Mol Cancer Ther 2015; 14: 847–856. [PubMed: 25695955]
28. Thorsson V, Gibbs DL, Brown SD, et al. The immune landscape of cancer. Immunity 2018; 48: 812–830. [PubMed: 29628290]
29. Kurnit KC, Kim GN, Fellman BM, et al. *CTNNB1* (beta-catenin) mutation identifies low grade, early stage endometrial cancer patients at increased risk of recurrence. Mod Pathol 2017; 30: 1032–1041. [PubMed: 28281553]
30. Myers A, Barry WT, Hirsch MS, et al. β-catenin mutations in recurrent FIGO IA grade 1 endometrioid endometrial cancers. Gynecol Oncol 2014; 134: 426–427. [PubMed: 24952365]
31. Spranger S, Bao R, Gajewski TF. Melanoma-intrinsic β-catenin signaling prevents anti-tumor immunity. Nature 2015; 523: 231–235. [PubMed: 25970248]

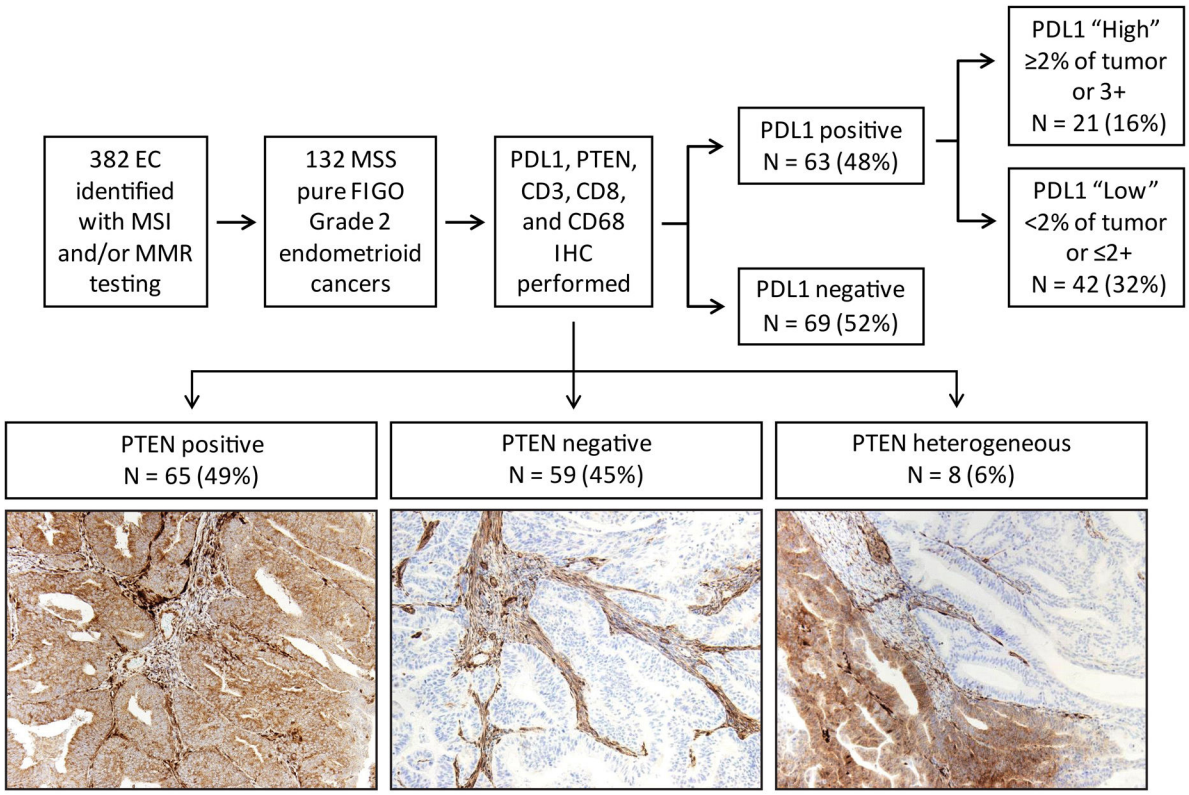

Figure 1.

Schematic overview of study design. A total of 382 endometrial cancers were tested for mismatch repair immunohistochemistry and/or PCR-based microsatellite instability analysis. From this group, 132 FIGO grade 2, microsatellite-stable endometrial cancers with intact expression of mismatch repair proteins were identified. PD-L1, PTEN, CD3, CD8, and CD68 immunohistochemical analyses were performed in this set of tumors.

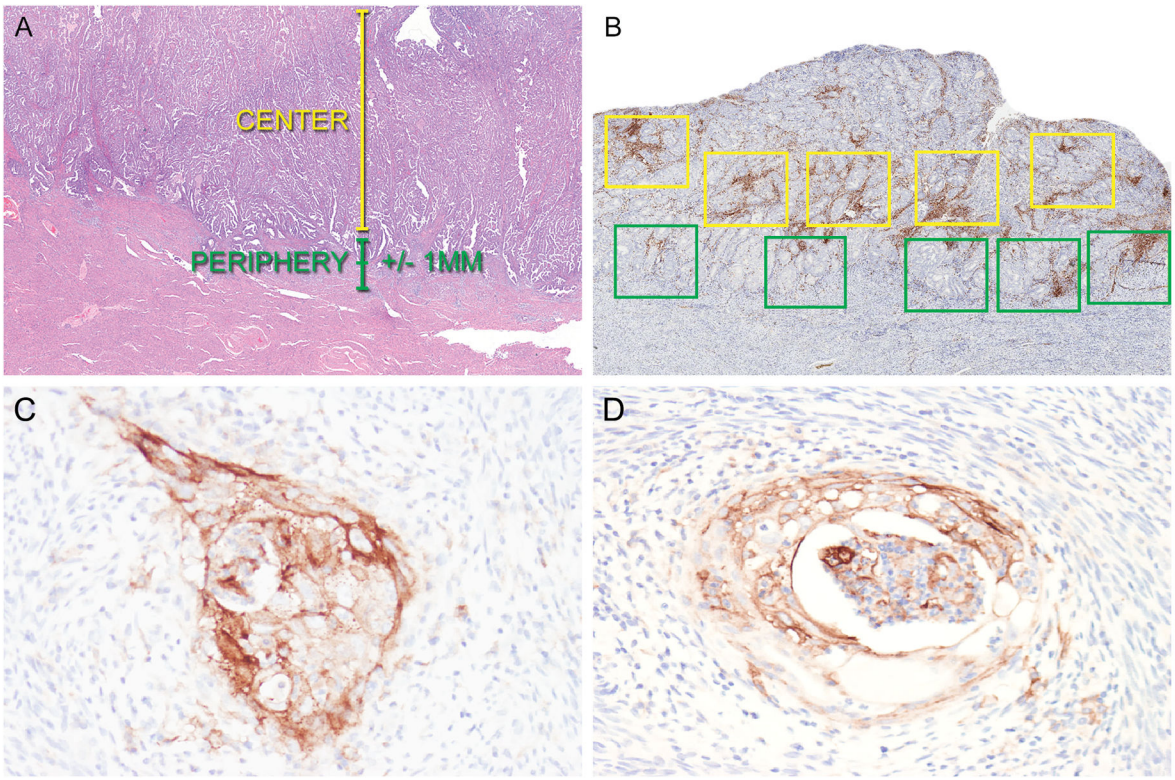

Figure 2.

Photomicrographs demonstrating approach for quantification of tumor-associated lymphocytes and macrophages (A and B) and representative examples of PD-L1 expression in endometrioid endometrial adenocarcinoma (C and D). A. Representative H&E of an endometrial cancer to demonstrate definitions of tumor center and periphery. B. Quantification of CD3+, CD8+, and CD68+ cells in the tumor center and periphery was performed using Aperio whole slide imaging software. Five 1 mm^2 boxes were placed at the tumor center (yellow boxes) and periphery (green boxes) in the areas of highest staining density by morphologic examination. Following quantification of positive cells in each box, mean positive cells/mm^2 was calculated for the tumor center and periphery. C. Positive PD-L1 expression in the invasive front of an endometrial cancer. D. Positive PD-L1 expression in foci of squamous metaplasia in an endometrial cancer.

Table 1.

Clinical and Pathological Characteristics of Mismatch Repair Intact Endometrial Carcinoma Cohort

Characteristics (n=132)	**Value**
Age, median (range), years	60 (27-88)
Tumor size*, median (range), mm	35 (10-145)
FIGO tumor stage, n (%)	
I	112 (85)
II	5 (4)
III	13 (10)
IV	2 (1)
Any myometrial invasion, n (%)	
Yes	95 (72)
No	37 (28)
Myometrial invasion ≥50%, n (%)	
Yes	30 (23)
No	102 (77)
Lymphovascular space invasion, n (%)	
Yes	30 (23)
No	102 (77)
Metastasis to pelvic lymph nodes, n (%)	
Yes	11 (8)
No	77 (58)
Lymph node dissection not performed	44 (33)
Metastasis to para-aortic lymph nodes, n (%)	
Yes	5 (4)
No	46 (35)
Lymph node dissection not performed	81 (61)
PTEN immunohistochemistry	
Positive	65 (49)
Heterogeneous	8 (6)
Negative	59 (45)

Table 2.

Clinical and Pathological Characteristics Associated with Tumor PD-L1 Positivity in Mismatch Repair Intact Grade 2 Endometrial Endometrioid Adenocarcinoma

Variable	Tumor PD-L1 negative (69/132; 52%)	Tumor PD-L1 positive (63/132; 48%)	*p*-value
Age, n, years			
Mean (SD)	59 (12)	59 (11)	0.857
Median (Minimum-Maximum)	60 (27-82)	60 (30-88)	
Tumor size (mm), n (%)			
Mean (SD)	43 (26)	47 (27)	
Median (Minimum- Maximum)	35 (13-127)	43 (10-145)	0.202
Tumor stage, n (%)			
I or II	66 (96)	51 (81)	0.012
III or IV	3 (4)	12 (19)	
Any myometrial invasion, n (%)			
Yes	44 (64)	51 (81)	0.028
No	25 (36)	12 (19)	
Myometrial invasion present and ≥50%, n (%)			
Yes	7 (16)	23 (45)	**0.002**
No	37 (84)	28 (55)	
Not applicable (no myometrial invasion)	25	12	
LVSI, n (%)			
Yes	8 (12)	22 (35)	**0.001**
No	61 (88)	41 (65)	
Metastasis to pelvic lymph nodes, n (%)			
Yes	2 (5)	9 (18)	0.105
No	36 (95)	41 (82)	
Metastasis to para-aortic lymph nodes, n (%)			
Yes	0	5 (15)	0.156
No	17 (100)	29 (85)	
PTEN IHC, n (%)			
Positive	42 (61)	23 (37)	
Heterogeneous	2 (3)	6 (10)	0.012
Negative	25 (36)	34 (54)	
CD3 (mean cells/mm^2, SD)			
Overall	800 (470)	989 (642)	0.110
Hotspot	1287 (688)	1647 (622)	0.024
Periphery	729 (436)	1087 (746)	0.003
Center	811 (516)	920 (627)	0.367
CD8 (mean cells/mm^2, SD)			
Overall	398 (293)	571 (548)	0.137
Hotspot	652 (441)	950 (733)	0.017
Periphery	383 (275)	654 (604)	0.010

Variable	**Tumor PD-L1 negative (69/132; 52%)**	**Tumor PD-L1 positive (63/132; 48%)**	***p*-value**
Center	379 (319)	508 (548)	0.323
CD68 (mean cells/mm^{2,} SD)			
Overall	176 (158)	179 (116)	0.315
Hotspot	286 (241)	308 (182)	0.118
Periphery	157 (152)	179 (120)	0.058
Center	193 (183)	183 (131)	0.696

Table 3.

Clinical and Pathological Characteristics Associated with High Tumor PD-L1 Positivity in Mismatch Repair Intact Grade 2 Endometrial Endometrioid Adenocarcinoma

Variable	Tumor PD-L1 negative (69/132; 52%)	Tumor PD-L1 high positive (21/132; 16%)	*p*-value
Age in years			
Mean (SD)	59 (12)	56 (12)	0.260
Median (Minimum-Maximum)	60 (27-82)	59 (30 – 77)	
Tumor size (mm)			
Mean (SD)	43 (26)	35 (17)	
Median (Minimum- Maximum)	35 (13-127)	31(12-75)	0.355
Tumor stage, n (%)			
I or II	66 (96)	18 (86)	0.735
III or IV	3 (4)	3 (14)	
Any myometrial invasion, n (%)			
Yes	44 (64)	18 (86)	0.065
No	25 (36)	3 (14)	
Myometrial invasion present and ≥50%, n (%)			
Yes	7 (16)	8 (44)	0.017
No	37 (84)	10 (56)	
Not applicable (no myometrial invasion)	25	3	
LVSI, n (%)			
Yes	8 (12)	8 (38)	0.005
No	61 (88)	13 (62)	
Metastasis to pelvic lymph nodes, n (%)			
Yes	2 (5)	3 (18)	0.165
No	36 (95)	14 (82)	
Metastasis to para-aortic lymph nodes, n (%)			
Yes	0	2 (18)	0.146
No	17 (100)	9 (82)	
PTEN IHC, n (%)			
Positive	42 (61)	8 (38)	
Heterogeneous	2 (3)	1 (5)	0.148
Negative	25 (36)	12 (57)	
CD3 (mean cells/mm^2, SD)			
Overall	800 (470)	1174 (724)	0.014
Hotspot	1287 (688)	1963 (895)	**0.001**
Periphery	729 (436)	1214 (749)	**0.002**
Center	811 (516)	1134 (766)	0.066
CD8 (mean cells/mm^2, SD)			
Overall	398 (293)	804 (755)	.017
Hotspot	652 (441)	1233 (859)	**0.001**
Periphery	383 (275)	882 (782)	0.003

Variable	**Tumor PD-L1 negative (69/132; 52%)**	**Tumor PD-L1 high positive (21/132; 16%)**	***p*-value**
Center	379 (319)	720 (782)	0.073
CD68 (mean cells/mm^2, SD)			
Overall	176 (158)	170 (106)	0.650
Hotspot	286 (241)	287 (159)	0.499
Periphery	157 (152)	171 (109)	0.231
Center	193 (183)	170 (118)	0.963

Table 4.

Effect of PTEN status on Tumor-Associated Immune Cell Infiltrates

Variable	Tumor PTEN Negative (59/132; 45%)	Tumor PTEN Positive/Heterogeneous (73/132; 55%)	*p*-value
CD3 (mean cells/mm^2, SD)			
Overall	879 (556)	899 (575)	0.967
Hotspot	1466 (777)	1454 (868)	0.714
Periphery	908 (575)	900 (678)	0.517
Center	846 (588)	879 (562)	0.643
CD8 (mean cells/mm^2, SD)			
Overall	462 (411)	495 (464)	0.969
Hotspot	781 (596)	803 (631)	0.998
Periphery	507 (472)	526 (500)	0.844
Center	413 (404)	464 (481)	0.912
CD68 (mean cells/mm^2, SD)			
Overall	194 (159)	163 (119)	0.332
Hotspot	324 (232)	274 (196)	0.175
Periphery	182 (144)	156 (130)	0.219
Center	204 (182)	175 (137)	0.560